

## INSURED LOSS ESTIMATION FROM WIND AND STORM SURGE FOR A RE-OCCURRENCE OF TYPHOON VERA

Peter J. Sousounis\* and Cagdas Kafali  
AIR Worldwide Corporation, Boston, MA

### 1. INTRODUCTION

Typhoon Vera (aka Isewan) struck Japan on September 26 1959, making landfall just west of Ise Bay (cf. Fig. 1 – upper panel) with maximum (10-min) sustained wind speeds of  $45.4 \text{ ms}^{-1}$  (maximum instantaneous wind speed was  $55.3 \text{ ms}^{-1}$ ) in Irako (Atsumi-cho, Aichi Prefecture),  $37.0 \text{ ms}^{-1}$  (maximum instantaneous wind speed  $45.7 \text{ ms}^{-1}$ ) in Nagoya, and over  $20 \text{ ms}^{-1}$  (maximum instantaneous wind speed over  $30 \text{ ms}^{-1}$ ) in almost every part of Japan from Kyushu to Hokkaido. The extraordinary high surge of up to 3.45 m that occurred around 9:30 pm LST (Kawai, 1999) tore down dykes along the coast and at river mouths. Flooding extended inland more than 20 km (cf. Fig. 1 – lower panel). Inundated areas, which were at low elevations and very flat, were slow to drain and it took days to weeks for the land to finally dry completely (Oda 2006). It killed 5,098 and injured 38,921, and caused an estimated 14 B USD insured damage (AXCO 2009). Typhoon Vera remains the worst typhoon disaster in Japan's recent history.

This paper presents hazard and loss results using simulations of Typhoon Vera if it were to re-occur today. The wind simulation was performed using a Typhoon Windspeed Model developed at AIR (JTM). The storm surge simulation was performed with a version of the Princeton Ocean Model (POM). Insured losses were computed for residential, commercial, industrial and automobile lines of business from an Industry-wide Exposure Database (IED) created at AIR.

### 2. HAZARD METHODOLOGY AND INITIAL CONDITIONS

The wind speed, surge height, and current velocities that were used to model the loss from Typhoon Vera were created using best track data from the Japanese Meteorological Agency as input to JTM. The POM was then used with this wind input along with other data for initial and lateral boundary conditions to generate surge heights and current velocities along the coast and over the land it inundated. These surge heights and current velocities from the POM were converted to surge depths using high resolution terrain data. The high resolution surge depths

and current velocities were then used to estimate damage and loss from surge.

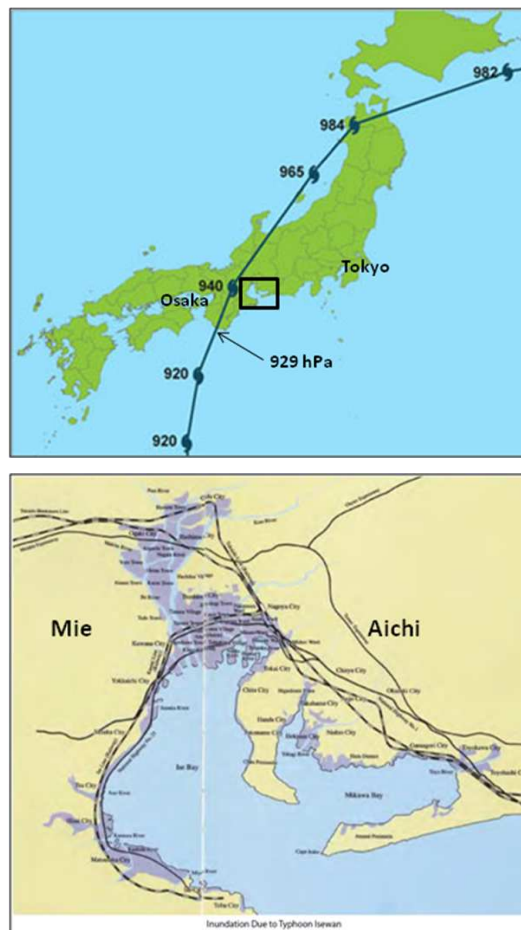


Fig. 1. Path and extent of inland flooding from Typhoon Vera.

#### 2.1 AIR Japan Typhoon Model

The wind speeds used to force the POM and to calculate wind damage to the industry exposure were generated using an updated version of the AIR Japan Typhoon Model (JTM). This model computes a gradient wind field based on specified values of central pressure and radius of maximum winds and uses a radial decay profile based on Willoughby et al. (2006). Surface winds are then computed using one kilometer elevation and land use / land cover (LULC) data obtained from the Japanese Ministry for Land Infrastructure and Transportation. Much

\* Corresponding author address: Peter J. Sousounis, AIR-Worldwide Corporation., 131 Dartmouth Street, Boston, MA 02116; email: psousounis@air-worldwide.com.

of the specific information for JTM is proprietary and cannot be described here.

## 2.2 Princeton Ocean Model

The Princeton Ocean Model (POM) is a free-surface, three-dimensional finite-difference numerical model based on the primitive equations with Boussinesq and hydrostatic approximations. The POM was originally developed in the mid 1980s (Blumberg and Mellor 1987) but continues to be upgraded. The POM has since come to include new features such as free surface to handle tides, sigma vertical coordinates (i.e., terrain-following) to handle complex topographies and shallow regions, a curvilinear grid to better handle coastlines, and a turbulence scheme to handle vertical mixing.

The POM has been used extensively to simulate and predict oceanic currents, temperatures, salinities and storm surges (Aoki and Isobe 2006; Chu et al. 2000, 2001; Chu and Fan 2001; Kohno and Higaki 2006; Minato 1996, 1998; Peng et al 2006; Ezer 2005, 2006; Ezer and Mellor 2004; Korres et al. 2007; Guo et al. 2004; Hong and Yoon 2003, Kim and Yamashita 2003). While the POM by itself has the capability to compute storm surge heights at coastal locations, a wetting and drying (WAD) scheme recently implemented (Oey 2005, 2006) allows water to inundate previously dry areas during a simulation. This capability enhances the model utility for determining areas that get flooded from storm surge. Vertical drainage of water into the ground, either naturally or through sewer or storm sewer systems is not included.

Implementation of the model for our purposes included defining a rectilinear coordinate grid with grid spacing 0.0041667 degree spacing between grid points and 400 points in the x-direction and 392 points in the y-direction and 16 vertical levels. The domain used in the POM simulations is shown in Fig. 2. Note that while this domain does not capture the full extent of the Aichi and Mie Prefectures, surge magnitudes at the far extents of the domain were minimal to nonexistent. Note also that for wind loss calculations, the full extent of the prefectures was included because the calculations were performed within the AIR Japan Typhoon Model. The model was initialized using bathymetry data and wind and sea level pressure fields as described below. An astronomical tidal cycle was also implemented.

## 2.3 Bathymetry

The bathymetry grid was created using a blend of two arc minute data from the National

Geophysical Data Center (NGDC - <http://www.ngdc.noaa.gov/mgg/image/2minrelief.html>) and 50 m elevation data from the Geographical Survey Institute (GSI - <http://www.gsi.go.jp/geoinfo/dmap/dem50m-index.html>). To these data was added levee and sea-wall information obtained by request from the Central Disaster Prevention Council (CDPC) of the Japan Cabinet Office.

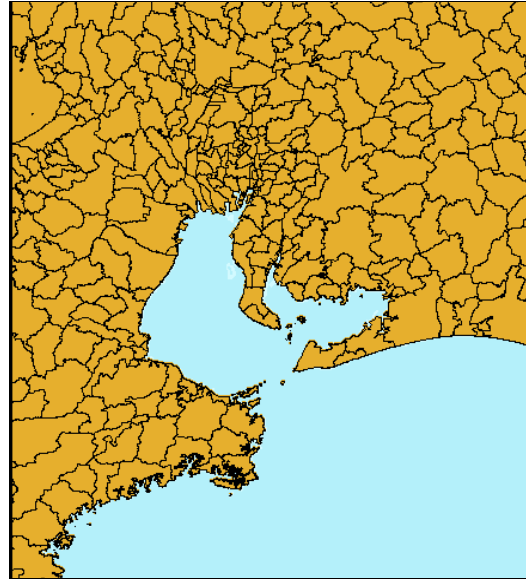


Fig. 2. Extent of POM domain used for Typhoon Vera storm surge simulations.

The NGDC data was interpolated to 0.0041667 degree resolution (~400 m resolution) onto a rectilinear bathymetry grid where sea water exists. The GSI 50 m resolution elevation data with CDPC levee height information was reduced to 0.0041667 degree resolution over land. The resulting bathymetry grid that was created was 400 points in the east-west direction and 392 points in the north-south direction starting at a southwest corner of: (136.112533569W, 33.983333588N). The resulting terrain and bathymetry is shown in Fig. 3. Figure 5b (upper) indicates the location of the Levee information by grid cell. Figure 3 (upper panel) shows the resulting terrain and bathymetry for Ise Bay after incorporation of the levee information. Figure 3 (lower panel) shows the grid-cell result of the sea-wall and levee information across the northern part of Ise Bay.

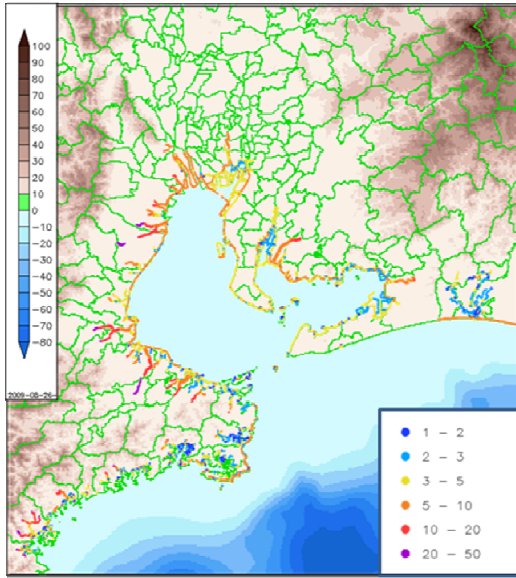


Fig. 3. Extent of POM domain used for Typhoon Vera storm surge simulations. Terrain and bathymetry are shaded (m). Levee heights (m) are shown as colored dots.

#### 2.4 Surface Winds

Wind forcing for the POM-WAD was provided from the JTM. Typhoon Vera was simulated with meteorological conditions close to those specified by the Japanese Meteorological Agency (JMA). Specifically, adjustments were made to the radius of maximum winds based on observational evidence from existing AMeDAS (Automated Meteorological Data Acquisition System) wind reports.

Typhoon Vera made landfall well to the west of Ise Bay and travelled northeastward – passing well to the north of Ise Bay. Despite its distance from Ise Bay, its path and a 929.5 hPa central pressure at landfall resulted in strong winds that were directed over a long fetch of the Bay towards a shallow narrow section of the Bay to the north. Additionally, the high forward speed towards the northeast contributed to the strong winds on the right hand side of the storm, where typhoons typically exhibit their strongest winds. The maximum windspeed footprint is shown in Fig. 4.

The JTM generated hourly wind fields at one-kilometer resolution over all of Japan – in order to account for wind damage in areas well away from the coast where storm surge could occur. Over the POM domain, however, the u- and v- wind components were interpolated to 0.0041667 degree resolution at 15-minute intervals for use in the POM. Additionally, a sea level pressure field was synthesized for input into POM in order to simulate the inverse barometer

effect. The pressure field was generated using the central pressure, radius of maximum winds, and a well known formula (Holland 1980).

### 3. STORM SURGE RESULTS

Two different levee configurations are analyzed here. The first one represents the situation that exists currently (InTactLevee) and the second represents a situation that could exist should a strong surge cause severe damage to the levees (BreachLevee). The BreachLevee configuration was created by evaluating results from the InTactLevee Simulations and removing a section of the InTactLevee configuration in the area where the highest surge occurred and replacing it with the corresponding NoLevee configuration (not shown).

A comparison of the InTactLevee, and BreachLevee bathymetry in the vicinity of the imposed breach is shown in Fig. 5. Note that the InTactLevee and BreachLevee configurations contain the seawall across Nagoya Harbor.

#### 3.1 Typhoon Vera 1959 InTactLevee Simulation

This simulation is close to a re-simulation of Typhoon Vera in 1959 with two exceptions. The big exception is that the terrain and levee elevation is not necessarily a true reflection of what existed at the time Typhoon Vera occurred. A second exception is that the astronomical tidal cycle used is meant to simulate the normal tidal cycle and not the muted one that actually occurred during the time of Typhoon Vera.

The results for the InTactLevee simulation (Fig. 6) show that maximum surge (defined as the maximum water height above undisturbed sea-level) occurred as the storm was passing well to the north of Ise Bay - as is demonstrated by the surface air wind vectors. Because of the prevailing southwesterly winds at the time of

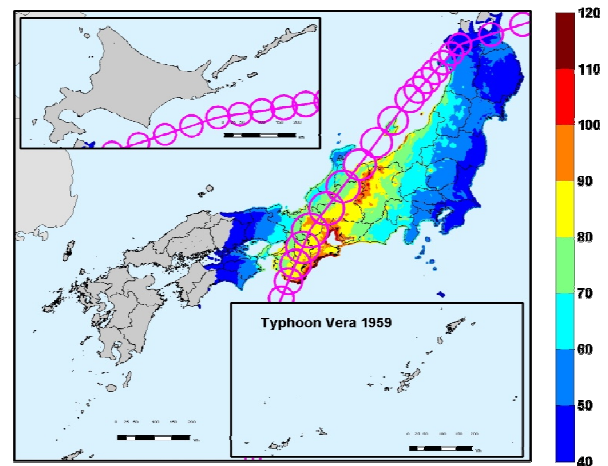


Fig. 4. Maximum sustained windspeed (mph) footprint for Typhoon Vera using JTM. Circles indicate hourly positions and radii of maximum winds.



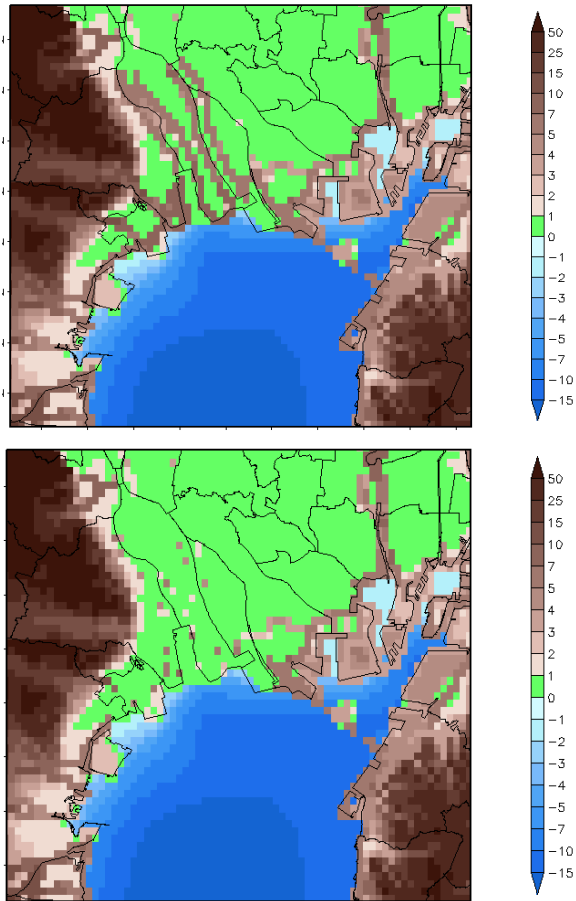


Fig. 5. Comparison of levee heights used in the InTactLevee and BreachLevee simulations with POM.

maximum surge, the storm really only affected Ise Bay and not Mikawa Bay (the smaller bay to the east). Maximum current speeds of surge water exceeded 3 m/s (not shown) and the maximum flood footprint extended 20 km or so inland (Fig. 8).

The 4.2 m surge height (cf. Fig. 7) compares favorably with the observed maximum surge height during Typhoon Vera of 3.89 m. Specifically, the maximum from Typhoon Vera in 1959 likely occurred in the presence of some levee and dyke barriers. The higher-than-observed surge in the InTactLevee Simulation is likely the result of a higher astronomical tide<sup>1</sup> than was observed at the time. Note also the good agreement between the maximum height in the surge-only simulation of 3.4 m and the

<sup>1</sup> Note that the tidal cycle at the location shown appears as a pulse because the model has not spun-up by the time the maximum surge occurs but is nonetheless and otherwise a realistic contribution. The typical two cycles/day oscillation does exist farther south in the bay.

estimated surge-only component of Typhoon Vera of 3.55 m. The difference may be the result of omitting the explicit contribution from wave set-up in our simulations. Finally, with respect to the time series at 35.05N, 136.716E, note that the sum of the maximum tide-only (e.g., astronomical tide) contribution and the maximum surge-only (e.g., meteorological or storm tide) is greater than the result when both are simultaneously included in the POM. This suggests some nonlinear interaction that acts to reduce the total relative to the sum of the parts – at least in the model. It is also possible that if the tide-only component were allowed to spin-up and/or were incorporated in a more sophisticated manner that the nonlinear effect would be reduced or eliminated

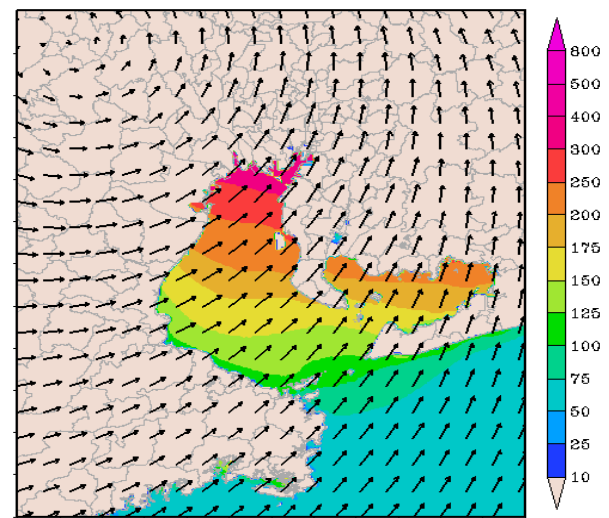


Fig. 6. Storm surge (shaded, cm) and surface winds (arrow) at  $t = 10$  h into simulation.

Inspection of Fig. 8 indicates that with minor exceptions the current levee system is sufficient to withstand a repeat of Typhoon Vera. The

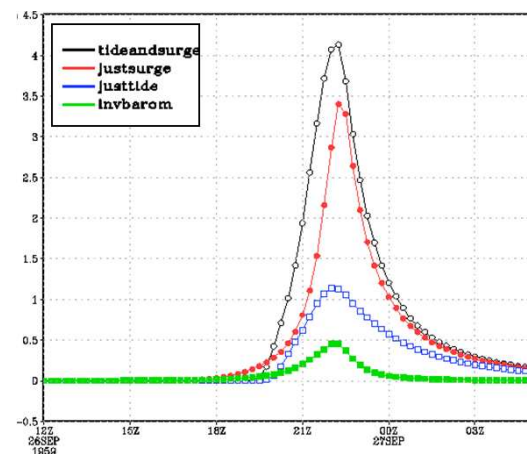


Fig. 7. Time series for component contributions (m) to InTactLevee storm surge height.

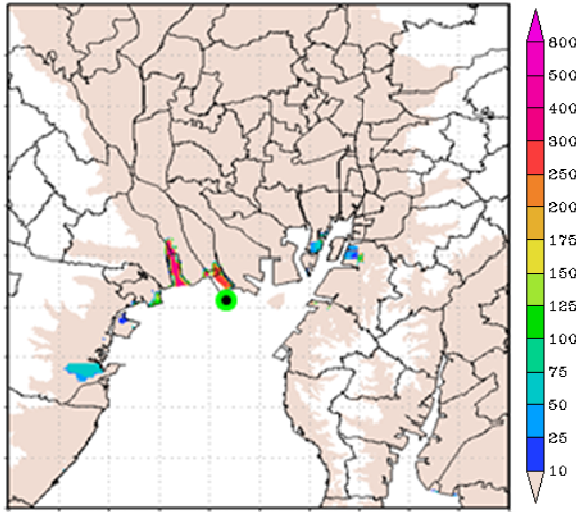


Fig. 8. Maximum inland flood depth (cm) from InTactLevee simulation. Circle indicates location of time series in Fig. 7.

resulting inland flooding in this simulation is negligible. Despite the 4.2 m peak surge, levee heights at that location are 5-7 m and because the levee is not breached, the water does not get past, except in only a few isolated locations.

### 3.2 Typhoon Vera 1959 BreachLevee Simulation

This simulation was performed to evaluate the impact of a recurrence of Typhoon Vera should the current levee system fail. The breach that was imposed and which was described earlier in Section 3 exists for the entire simulation. Thus, water is allowed to flow freely from the time it reaches the area of the breach. In this sense the simulation is more similar to the NoLevee Simulation (not shown in this study). Results for this simulation are shown in Figs. 9-11. For example, in the area just north of Ise Bay and west of Minato Ward, water has already inundated the land (by  $t=10$  h) to a considerable extent. The area east of Minato Ward remains dry, primarily because the seawall south of there remains intact. Figure 10 shows that maximum current velocities are on the order of 2.5 – 3 m/s.

Figure 11 illustrates the extent of the flooding. North of Ise Bay, flooding extends as far north as it does in the NoLevee Simulation but not as far east. Flooding is restricted to the region fanning outward and upward from the breach. A sharp boundary defines the eastern boundary of the flooding. In addition to the areal extent, flood depths in the areas that are flooded, are comparable to those in the NoLevee Simulation. The far northward extent and depth of the flooding supports the notion that restriction in the size of the breach may not necessarily prevent extensive flooding from occurring.

## 4. IMPACT ON LOSSES

Nagoya City is the capital of Aichi Prefecture. It is the third-largest city and fourth most populous urban area in Japan and one of Japan's major ports. It is also the center of Japan's third largest metropolitan region - the Chukyo Metropolitan Area, which has 8.74 million people, 2.17 million of which live in Nagoya City (as of 2000). Much of Nagoya city is at or below mean sea level. The 2007 industry exposure distribution was created at AIR using a combination of census, satellite, and economic data using proprietary techniques developed at AIR. The distribution is shown in Fig. 12. Partitioning by construction type and Line-of-Business (LOB) was also performed owing to the fact that damage functions, which relate windspeed or flood depth to fractional damage, depend on these characteristics (cf. Fig. 13).

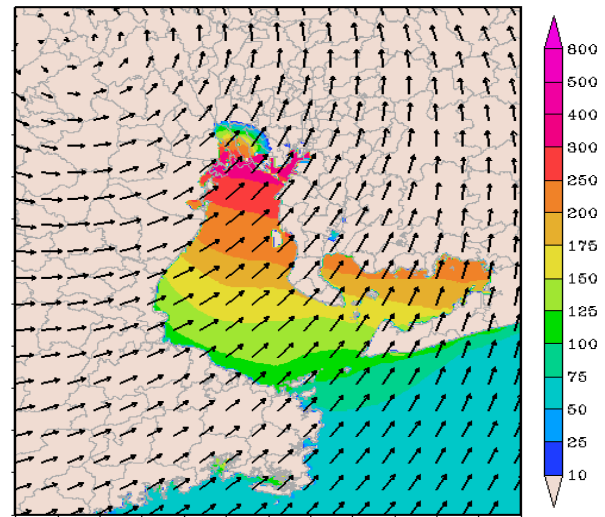


Fig. 9. Storm surge (shaded, cm) and surface winds (arrow) at  $t = 10$  h into InTactLevee simulation.

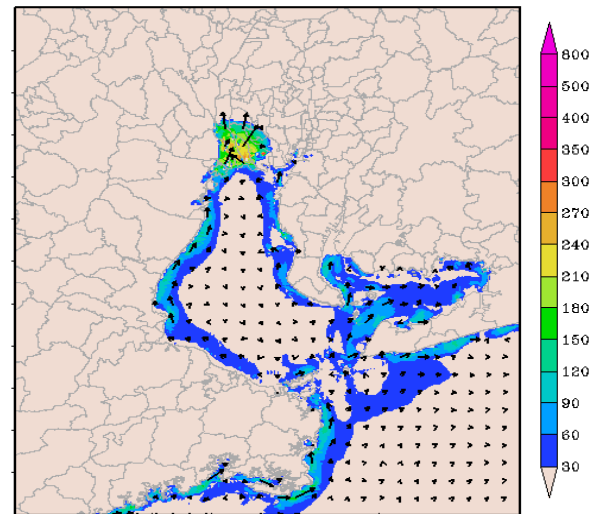


Fig. 10. Current speeds (shaded, cm/s) and mean current velocities (arrows) at  $t = 10$  h into InTactLevee simulation.

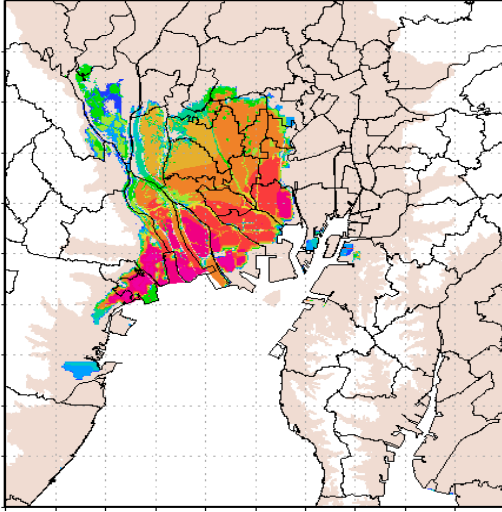


Fig. 11. Maximum inland flood depth (cm) from Breach Levee simulation. See Fig. 9 for legend.

#### 4.1 damage functions

In this section we (1) briefly discuss how the losses are calculated given the hazard results from Section 3 and the exposure information and policy terms, (2) summarize observed damage and losses from 1959 Typhoon Vera, and (3) present model losses for the InTactLevee scenario.

Damage functions are relationships between hazard parameters and damage to the relevant exposure (building, content, etc.). Figure 13 shows sample wind and flood damage functions for residential LOB. Additionally, separate wind and flood damage functions were developed for building, content, and business interruption risks.

Regarding damage from flood, the velocity of the water must be incorporated. A standard approach is to include the current as an increment to the flood depth. The “effective” flood depth, thus accounts for the flood depth and current speed observed (calculated) at a given location. It accounts for the hydrostatic and hydrodynamic loads acting on a structure. A relationship from ASCE7 2005, (Chapter 5, Eq. 5.1) is used in this study to obtain the effective flood depth  $H_{eff}$ ;

$$H_{eff} = H_{max} + a \cdot V_{max}^2 / (2 \cdot g),$$

where  $H_{max}$  and  $V_{max}$  are maximum flood depth and maximum current velocity at a location obtained in previous sections,  $a$ =drag coefficient (here we have used  $a=1.5$ ) and  $g$ =acceleration of gravity. The above equation holds when water velocity does not exceed 3.05 m/sec, which is the case for all the grid points in all simulations in the previous section, except for very few instances.

The amount of damage for a given hazard level is generally uncertain. Accordingly, we define the damage ratio as a random variable and the mean of the damage ratio, for a given hazard level, is obtained from damage functions, such as those shown in Fig. 13. However, for the complete definition of the damage ratio, a probability distribution function is required. We have used a non-parametric distribution function, which is in turn a function of the mean damage ratio, to define the probability law of the damage ratio. This distribution also allows us to apply appropriate policy conditions and calculate gross losses, from the ground-up (before applying policy terms) losses.

#### 4.2 Model Losses

Losses for the BreachLevee simulation were computed. Wind losses were computed for all of Japan using the windspeeds and durations obtained from JTM. Flood losses were computed

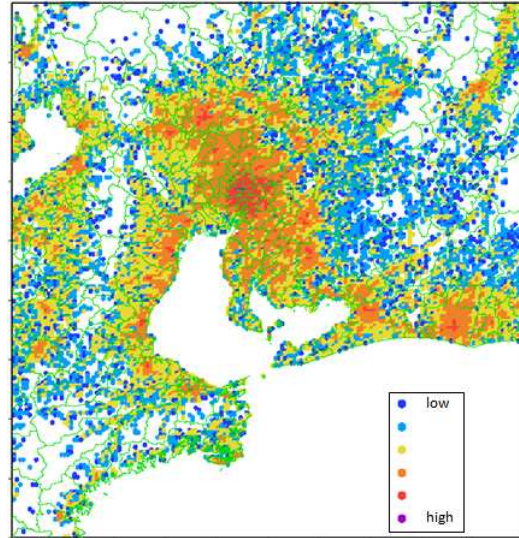


Fig. 12. Industry exposure distribution surrounding Ise Bay.

in Aichi and Mie prefectures using the information from the POM simulation. Policy conditions (e.g., deductibles, limits) are applied to obtain insured loss estimates. The results are shown in Table 1 and are broken down by peril and contribution from Aichi and Mie prefectures. The estimated total insured loss for Japan is 17.9 B USD. Surge contributes about 20% of the total loss for all of Japan. But, in Aichi and Mie Prefectures, the ratio of surge to wind loss is ~ 2:1.



Peril	Aichi/Mie	All Japan
Wind	1.9	14.1
Flood	3.8	3.8
Total	5.7	17.9

Table 1. Summary of computed losses from a re-occurrence of Typhoon Vera – BreachLevee scenario. Losses are in B USD (assuming 100 JPY = 1 USD)

The computed loss from the InTactLevee scenario is in agreement with published values from other sources. For example, AXCO reports that a recurrence of 1959 Typhoon Isewan would cause an estimated 14 bn USD loss to the insurance industry (approximately 1400 bn JPY using 1USD=100JPY) (AXCO 2009). Another report suggests that this value would be closer to 15bn USD (Lloyd's 2009). In (Yamamoto and Iwaya, 2002) it is reported that the amount of flood damage in Aichi prefecture alone from Typhoon Isewan was 322 bn JPY, however no specifics were provided (such as, if the loss was from residential damage only, or if it included losses to the infrastructural system, etc.).

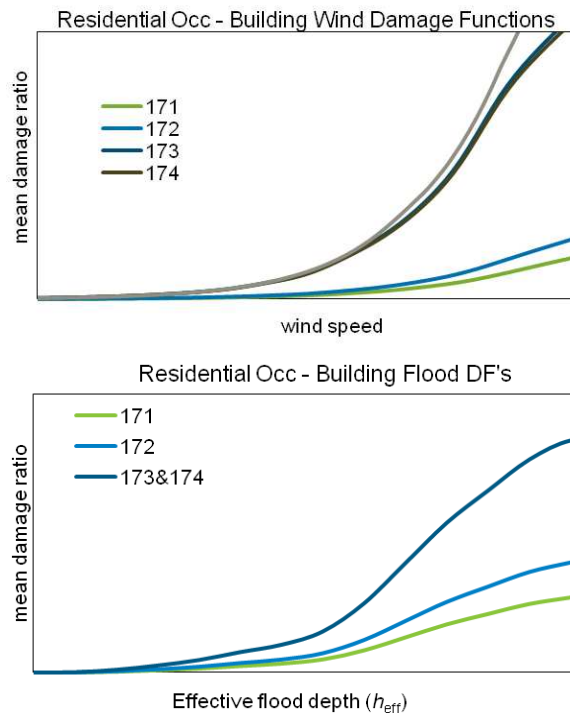


Fig. 13. Examples of wind and flood damage functions developed at AIR for different construction types.

## 5. CLOSING REMARKS

The results presented in this report provide expected insured loss information given a re-occurrence of Typhoon Vera using the InTactLevee scenario. Evaluation of the event from the InTactLevee perspective also provides useful information in that it demonstrates the current levee system is sufficient to withstand storm surge damage if it is not damaged.

The storm surge modeled in this study includes the primary contribution from wind stress (e.g., the wind set-up portion). It also includes that from the low atmospheric pressure (inverse barometric effect), as well as the contribution from astronomical tide. The fact that these Simulations were additionally conducted with forced simultaneity of high tide makes the events that much more rare to occur. An explicit account for wave set-up was not possible with the wave model that was proposed, however a theoretical estimate indicates that it is not the primary contributor to the storm surge, although it is likely not insignificant. This study also did not include effects of wave run-up, which likely would be less than those from wave set-up. To demonstrate what a significantly higher surge height (e.g., from including wave set-up) could do, an additional simulation with a high maximum drag coefficient was run. Assuming the current levee system can hold, even this significantly higher surge height would cause minor flooding and losses.

Finally, and most importantly, we note that the estimated storm surge loss computed here depends on the prescribed levee breach. The prescribed breach was so specified because of where the greatest surge height occurred in the InTactLevee simulation but a slightly different storm track, etc may lead to greastest surge height elsewhere. For example, a breach farther east and closer to Nagoya City could likely result in greater loss. Thus, to truly obtain useful loss information an ensemble of breach scenarios along with their likelihood of probabilities, would need to be created, simulated, and evaluated.

## Acknowledgements

We gratefully acknowledge the availability and use of levee data from the Central Disaster Prevention Council of the Japan Cabinet Office in Tokyo, Japan.

## REFERENCES

Aoki, K. and A. Isobe , 2006: Numerical study of the summer temperature decrease induced by the enhancement of estuarine circulation in Fukuoka Bay, *Jour. Oceanogr.*, **62**, 207-217.

ASCE7, Minimum design loads for buildings and other structures, ASCE Standard ASCE/SEI 7-05, American Society of Civil Engineers, 2005.

AXCO, Insurance market report: Japan non-life (P&C), AXCO, 2009.

Blumberg, A.F., and G.L. Mellor, A description of a three-dimensional coastal ocean circulation model, in Three-Dimensional Coastal Ocean Models, Vol. 4, edited by N.Heaps, pp. 208, American Geophysical Union, Washington, D.C., 1987.

Chu, P. C., J. M. Veneziano, C. Fan, M. J. Carron, and W. T. Liu, 2000: Response of the South China Sea to Tropical Cyclone Ernie 1996, *J. Geophys. Res.*, 105(C6), 13,991–14,009.

Chu P. C. and Chenwu Fan, 2001: An Accuracy Progressive Sixth-Order Finite-Difference Scheme, *Jour. Atmos. Ocean. Tech.*, **18**, 1245–1257.

Chu, P. C., S. Lu, and Y. Chen, 2001: Evaluation of the Princeton Ocean Model Using South China Sea Monsoon Experiment (SCSMEX) Data, *Jour. Atmos. Ocean. Tech.*, **18**, 1521–1539.

Ezer, T., 2005: Entrainment, diapycnal mixing and transport in three-dimensional bottom gravity current simulations using the Mellor-Yamada turbulence scheme. *Ocean Modell.*, **9**, 151–168.

—, 2006: Topographic influence on overflow dynamics: Idealized numerical simulations and the Faroe Bank Channel overflow. *J. Geophys. Res.*, **111**, C02002, doi:10.1029/2005JC003195.

—, and G. Mellor, 2004: A generalized coordinate ocean model and comparison of the bottom boundary layer dynamics in terrain-following and in z-level grids. *Ocean Modell.*, **6**, 379–403.